

# Systematic investigation of nucleon optical model potentials in $(p, d)$ transfer reactions\*

Silu Chen (陈思璐)<sup>1</sup> Zixuan Liu (刘子旋)<sup>1</sup> Zhi Zhang (张智)<sup>2</sup> Ruirui Xu (续瑞瑞)<sup>2</sup>  
Danyang Pang (庞丹阳)<sup>3</sup> Yiping Xu (许祎萍)<sup>1†</sup>

<sup>1</sup>School of Nuclear Science and Engineering, North China Electric Power University, Beijing 102206, China

<sup>2</sup>China Nuclear Data Center, China Institute of Atomic Energy, Beijing 102413, China

<sup>3</sup>School of Physics, Beihang University, Beijing 100191, China

**Abstract:** The consistent three-body model reaction methodology (TBMRM) proposed by J. Lee *et al.* [1–3], which includes adopting the simple zero-range adiabatic wave approximation, constraining the single-particle potentials using modern Hartree–Fock calculations, and using global nucleon optical model potential (OMP) geometries, are widely applied in systematic studies of transfer reactions. In this work, we study the influences of different nucleon OMPs on extraction of spectroscopic factors (SFs) from  $(p, d)$  reactions. Our study covers 32 sets of angular distribution data of  $(p, d)$  reactions on 4 targets, as well as a large range of incident energies (20–200 MeV/nucleon). Two semi-microscopic nucleon OMPs, JLM [4, 5] and CTOM [6], and a pure microscopic nucleon potential WLH [7] are used in the present work. The results are compared with those using the phenomenological global optical potential KD02 [8]. We find the incident energy dependence of spectroscopic factors extracted from  $(p, d)$  reactions is obviously suppressed when microscopic OMPs are employed for  $^{12}\text{C}$ ,  $^{28}\text{Si}$  and  $^{40}\text{Ca}$ . In addition, spectroscopic factors extracted using the systematic microscopic optical potential CTOM based on the Dirac-Brueckner-Hartree-Fock theory are more in line with the results obtained from  $(e, e'p)$  measurements, except  $^{16}\text{O}$  and  $^{40}\text{Ca}$  at high energies ( $> 100$  MeV), calling for an exact treatment of double-magic nuclei. The results obtained by using pure microscopic optical potential WLH based on EFT theory shows the same trend but generally higher than CTOM. JLM potential, which relies on simplified nuclear matter calculations with old-fashioned bare interactions, produces very similar results with phenomenological potential KD02. Our results indicate that modern microscopic OMPs are reliable tools for probing the nuclear structure by transfer reactions across a wide energy range.

**Keywords:** optical model potentials, transfer reactions, spectroscopic factors

**DOI:**

## I. INTRODUCTION

Spectroscopic factors (SFs), which describe the strengths of single-particle states at the Fermi surface of shell closures or quasi-particles, are traditionally considered as a link between studies of nuclear reactions and nuclear structures [9]. For example, the quenching of SFs is an important subject (see review [10] and references therein), because it is generally suggested to originate from nucleon-nucleon (NN) correlations. Single nucleon transfer reactions, such as  $(p, d)$  and  $(d, p)$  reactions, which are main tools to extract SFs over the decades. However, the important question remains: the SFs extracted from transfer reactions show large uncertainties, which result from experimental measurements [11] and theoretical prediction [12–16]. The latter are typically as-

sociated with the choice of reaction models, optical model potentials (OMPs) and the single-particle potential (SPP) parameters. With the increasing interest in using single-nucleon transfer reactions to probe nuclear structure and astrophysical information, there is an ongoing need to evaluate the accuracy of the common methodology in transfer reactions throughout a wide energy range.

Aimed at this problem, J. Lee and J. A. Tostevin *et al.* developed a consistent three-body model reaction methodology (TBMRM) for the analysis of  $(p, d)$  and  $(d, p)$  reactions [1–3, 17, 18], which has been effectively improved the consistency of SFs extracted from transfer reactions. The methodology includes adopting the zero-range adiabatic wave approximation (ZR-ADWA) [19], constraining the SPP parameters by modern Hartree–Fock (HF) calculations, and using global nucleon optical po-

Received 16 September 2023; Accepted 23 April 2024

\* This work is supported by the National Natural Science Foundation of China (Grants Nos. U2067205, 12205098)

† E-mail: xuyip\_sne@ncepu.edu.cn

©2024 Chinese Physical Society and the Institute of High Energy Physics of the Chinese Academy of Sciences and the Institute of Modern Physics of the Chinese Academy of Sciences and IOP Publishing Ltd

tentials that can be applied consistently at all the required incident energies and for all targets, for example, OMPs derived by folding the effective nucleon-nucleon interaction of Jeukenne, Lejeune, and Mahaux (JLM) [4, 5] with the nucleon density distributions from the same HF calculations. However, there are some problems in widely applying this methodology to  $(p, d)$  and  $(d, p)$  reactions.

Firstly, most systematic analyses using the TBMRM are performed at relatively low energies (about 5-30 MeV/nucleon). Energy dependencies were noted for the SFs extracted from higher energy experimental data [20, 21], which is not as expected. Considering the energy-dependence of OMPs and the validity of adiabatic approximation [22, 23], it is essential to study the effects on the nuclear structure information extracted from experimental data within a wide energy range. In addition, according to our previous work, nucleon elastic scattering and transfer reactions are sensitive to different regions of the OMPs [24]. Therefore, global nucleon OMPs, which are primarily constrained with elastic scattering cross section, may not be sufficient for transfer reactions.

In our previous work [24], we suggested that microscopic OMPs, which reflect more theoretical considerations, should be preferred over phenomenological ones in calculations of direct nuclear reactions. In recent years, there are significantly more experimental data and microscopic OMPs available. For instance, a systematic microscopic optical potential CTOM was proposed by R. R. Xu *et al.* [6], which is based on the Dirac-Brueckner-Hartree-Fock theory. Lately, T.R. Whitehead, Y. Lim, and J.W. Holt constructed a microscopic global nucleon-nucleus optical potential based on an analysis of 1800 isotopes in the framework of many-body perturbation theory with a state-of-the-art nuclear interactions from chiral effective field theory (EFT) [7]. An attractive feature of the WLH potential is that none of its parameters are fitted to nucleon-nucleus scattering data. One might expect that, being derived fully microscopically, the new microscopic potential might be more suitable for probing nuclear structure information via transfer reactions, although OMPs with different parameter sets can usually reproduce the scattering cross section equally well. It is thus necessary to test the CTOM and WLH potential with  $(p, d)$  transfer reactions, to see how their results compare with the same calculations using phenomenological global nucleon-nucleus potentials. In addition, there are lack of research for transfer reaction beyond 70 MeV/nucleon, although most of global systematic OMPs for nucleons are valid up to 200 MeV/nucleon. Therefore, we analyze available experimental data, including 32 sets of  $(p, d)$  reactions angular distributions on  $^{12}\text{C}$ ,  $^{16}\text{O}$ ,  $^{28}\text{Si}$  and  $^{40}\text{Ca}$  for a range of incident energies up to 200 MeV/nucleon. Different types OMPs (three microscopic sets and one phenomenological sets) are applied in this work within the ADWA framework. Our goal in this paper is to investigate the effects

of different OMPs on the nuclear structure information extracted from  $(p, d)$  experimental data over a wide energy range.

## II. MODEL CALCULATIONS

Most of global systematic OMPs for nucleons used widely at present are limited to 200 MeV/nucleon. For this reason, experimental  $(p, d)$  differential cross sections data available below 200 MeV/nucleon are used to investigate the systematic behavior of SFs in a range of incident energy as wide as possible. They are for the reactions  $^{12}\text{C}_{\text{g.s.}}(p, d)^{11}\text{C}_{\text{g.s.}}$ ,  $^{16}\text{O}_{\text{g.s.}}(p, d)^{15}\text{O}_{\text{g.s.}}$ ,  $^{28}\text{Si}_{\text{g.s.}}(p, d)^{27}\text{Si}_{\text{g.s.}}$  and  $^{40}\text{Ca}_{\text{g.s.}}(p, d)^{39}\text{Ca}_{\text{g.s.}}$ . The choice of target nuclei is mainly limited by the applicability of method. As the HF is less appropriate for the description of single-particle configurations of very light systems, we limit the target masses to  $A > 11$ . In addition, the reaction mechanism of light nuclei is relatively simple. For example, in the light nuclei, the effect the spin-orbit interaction in constructing the valence neutron wave function is of the order of 10% or less [25]. And the availability of the experimental data is also taken into account, so we finally choose these four targets. The experimental data analyzed in this paper are listed in Table 2. All the experimental data were taken from the nuclear reaction database EXFOR/CSISRS [26] or digitized from their original references [27–32].

We have adopted and developed the three-body model reaction methodology (TBMRM) proposed by J. Lee *et al.* for the analysis of  $(p, d)$  reactions [2, 3, 18]. This methodology makes use of the Johnson-Soper ADWA model [19] for  $(p, d)$  and  $(d, p)$  reactions, with which, the amplitude of a  $A(p, d)B$  reaction reads [13]:

$$T_{pd} = S F_{nlj}^{1/2} \langle \chi_{dB}^{(-)} \phi_{np} | V_{np} | \chi_{pA}^{(+)} \phi_{nlj} \rangle, \quad (1)$$

where  $S F_{nlj}$  is the spectroscopic factor with  $n$ ,  $l$ , and  $j$  being the principal quantum number, the angular momentum and the total angular momentum, respectively, of the single neutron wave function  $\phi_{nlj}$  in the nucleus  $A$  ( $A = B + n$ ).  $\chi_{pA}$  and  $\chi_{dB}$  are entrance- and exit-channel distorted waves, and  $V_{np}$  is the neutron-proton interaction which supports the bound state of the  $n$ - $p$  pair  $\phi_{np}$  (the deuteron wave function).

With the finite-range (FR) ADWA model, the exit-channel distorted waves are generated with the following effective “deuteron” (as a subsystem composed of neutron and proton) potential [19, 33]:

$$U_{dB}(\mathbf{R}) = \frac{\langle \phi_{np} | V_{np} [U_{nB}(\vec{\mathbf{R}} + \frac{\vec{\mathbf{r}}}{2}) + U_{pB}(\vec{\mathbf{R}} - \frac{\vec{\mathbf{r}}}{2})] | \phi_{np} \rangle}{\langle \phi_{np}(\vec{\mathbf{r}}) | V_{np}(\vec{\mathbf{r}}) | \phi_{np}(\vec{\mathbf{r}}) \rangle} \quad (2)$$

where  $U_{nB}$  and  $U_{pB}$  are the neutron and proton optical

model potentials on the target nucleus  $B$  evaluated at half of the deuteron incident energies (the “ $E_d/2$  rule”). Thus, nucleon OMPs for the p- A, p-B, and n-B systems are needed in a  $A(p, d)B$  reaction.

In most of the previous work having applied TBM-RM, the zero-range (ZR) adiabatic potential is used in the ADWA calculations. In the zero-range version of the ADWA, the effective deuteron potential become simply:

$$U_{dB}(R) = U_{nB}(R) + U_{pB}(R) \quad (3)$$

However, the systematic calculations performed by Nguyen *et al.* [23] show that finite-range effects may become more significant with beam energies increased. Therefore, the finite-range version of adiabatic potential is applied in this work.

Table 1 shows all global systematics of nucleon OMPs used in this work to analyse the transfer data. Microscopic OMPs of JLM [4] and CTOM [6] are employed for proton and neutron potentials with nucleon density distributions given by HF calculations. The real and imaginary parts of the JLM potentials are scaled with the conventional factors  $\lambda_v = 1.0$  and  $\lambda_w = 0.8$  [2, 34]. Note that, although the WLH potential is supposed to work for incident energies below 150 MeV, our previous work shows it can reasonably reproduce the transfer data for higher energies at forward angles. For the same reason, we choose the global phenomenological OMP KD02.

For more realistic descriptions of the reaction mechanism, the optical potential should be non-local. Non-locality corrections with a range parameter of 0.85 fm obtained by fitting the experimental data, are included in the proton channel. The common deuteron potential non-locality correction parameter is not recommended in an adiabatic description of the deuteron channel, so the non-locality of the deuteron OMP is not taken into account in this work.

The single particle wave functions are calculated with the separation energy prescription with Woods-Saxon form of single particle potentials. The depths of these potentials are adjusted to reproduce the separation energies of the neutron in the ground states of the target nuclei. The radius and diffuseness parameters of these potentials,  $r_0$  and  $a_0$ , are also important for nuclear transfer reactions. Their empirical values are  $r_0 = 1.25$  fm and

$a_0 = 0.65$  fm. However, these empirical values can not be expected to represent the specific structure of any single specific nucleus. A better solution is to confine the  $r_0$  and  $a_0$  values with reliable nuclear structure theory. The TBM-RM constrains  $r_0$  and  $a_0$  values using modern Hartree-Fock (HF) calculations [18, 35–40]. With such a procedure, the diffuseness parameter is fixed to be  $a_0 = 0.65$  fm. The radius parameter  $r_0$  is determined by requiring the root mean square (rms) radius of the single neutron wave function,  $\sqrt{\langle r^2 \rangle}$ , being related with the rms radius of the corresponding single particle orbital from HF calculations,  $\sqrt{\langle r^2 \rangle}_{\text{HF}}$ , by  $\langle r^2 \rangle = [A/(A-1)]\langle r^2 \rangle_{\text{HF}}$ . The factor  $[A/(A-1)]$  is used for correction of fixed potential center assumption used in the HF calculations, where  $A$  is the mass number of the composite nucleus. All of HF calculations made in this work are based on the SkX interaction [41]. After  $r_0$  and  $a_0$  are determined, the depths of the single particle potentials are determined using experimental separation energies  $S_n^{\text{exp}}$ . All calculations make the local energy approximation (LEA) for finite range effects using the normalization strength ( $D_0 = -125.2$  MeV\*fm<sup>3/2</sup>) and range  $r(\beta = 0.7457$  fm) parameters of the Reid soft-core  ${}^3S_1$ - ${}^3D_1$  neutron-proton interaction. The computer code TWOFNR [42] is adopted for calculations of differential cross sections.

The theoretical calculations with different sets of optical parameters can reasonably reproduce the experimental data. By matching these theoretical differential cross sections to the former at the largest experimental cross sections, the experimental SFs,  $SF^{\text{exp}}$ , of the neutrons in the ground states of the reaction residues are obtained. In general, the experimental angular distributions at larger angles are more sensitive to details of the optical potential, the effects of inelastic couplings and other higher order effects that are not well reproduced by most reaction models. Furthermore, discrepancies between the shapes from calculations and experiment are much worse at the cross section minimum. Thus, the spectroscopic factor is generally extracted by fitting the reaction model predictions to the angular distribution data at the first peak, with emphasis on the maximum. The accuracy in absolute cross section measurements near the peak is most important. When possible, we take the mean of as many points near the maximum as we can to extract the spectroscopic factors. As an example, we show the analysis of the  ${}^{12}\text{C}(p, d){}^{11}\text{C}$  reaction at an incident energy of

**Table 1.** Global systematics of optical potentials for nucleons.

Projectile	Systematics	Type	Mass range	Energy range
$p, n$	JLM	semi-microscopic	$12 \leq A \leq 208$	$E \leq 200$ MeV
$p, n$	CTOM	semi-microscopic	$12 \leq A \leq 208$	$E \leq 200$ MeV
$p, n$	WLH	microscopic	$12 \leq A \leq 242$	$E \leq 150$ MeV
$p, n$	KD02	phenomenological	$24 \leq A \leq 209$	$E \leq 200$ MeV

30.3 MeV in Figure 1 to illustrate the procedure we adopt to extract the spectroscopic factors. In Figure 1, the first four data points with  $\theta < 30^\circ$  have been used to determine the ratios of the measured and calculated differential cross sections. The mean value of these four ratios is adopted as the experimental SF. The results are listed in Table 2.

The theoretical SFs and corresponding interactions used in the calculations are listed in Table 3. In this work, the theoretical spectroscopic factors  $SF^{th} = [A/(A-1)]^N \times C^2S(J^\pi, nlj)$ , where the shell model spectroscopic factors  $C^2S(J^\pi, nlj)$  are obtained from shell model calculations using the code OXBASH [43].  $J^\pi$  is the spin-parities of the core states, and  $nlj$  stand for the quantum numbers of the single particle states of the transferred nucleon. The factor  $[A/(A-1)]^N$  is for the center-of-mass corrections to the shell model SFs [44], where  $N = 2n + l$  is the number of the oscillator quanta associated with the major shell of the removed particle and  $A$  is the mass number of the composite nucleus.

### III. RESULTS AND DISCUSSIONS

As it is known, the SFs extracted from experimental data are quenched considerably as compared to the predictions of independent particle or shell models for nuclei. In transfer reactions, the reduction factors of single-nucleon strengths  $R_s$  are defined as the ratio between the experimental and theoretical SFs:  $R_s = SF^{exp}/SF^{th}$ . Such quenching of single particle strengths has been attributed to some profound questions in nuclear physics, such as short- and medium-range nucleon–nucleon correlations and long-range correlations from coupling of the single-particle motions of the nucleons near the Fermi surface

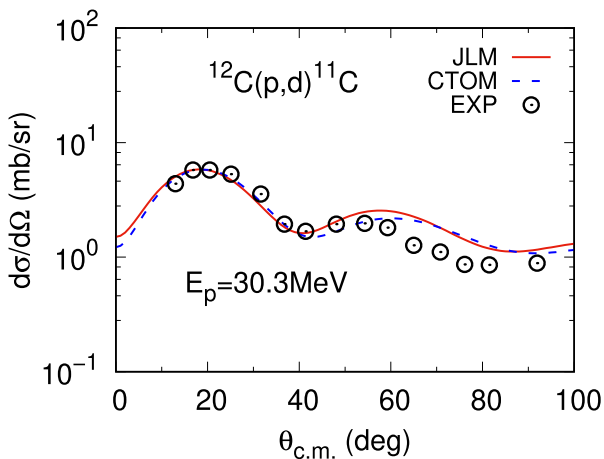


**Fig. 1.** (color online) The angular distributions  $^{12}C_{g.s.}(p,d)^{11}C_{g.s.}$  reaction at incident proton energy of 30.3 MeV [. The curve and dashed line are the theoretical results calculated by JLM and CTOM, multiplied by the corresponding spectroscopic factor, separately.

and the collective excitations. In addition, the reduction factors obtained from transfer [2, 18, 38, 39, 45–48], single-nucleon removal [35, 36, 40, 49–53] and quasi-free knockout [54–60] reactions show quite different dependence on proton-neutron asymmetry, which is still an open question [10].

Obviously, for transfer reactions, the uncertainties of  $R_s$  come from the extraction of experimental spectroscopic factors. As we know, the quenching of single-nucleon

**Table 2.** List of experimental spectroscopic factors extracted from  $(p,d)$  reactions.

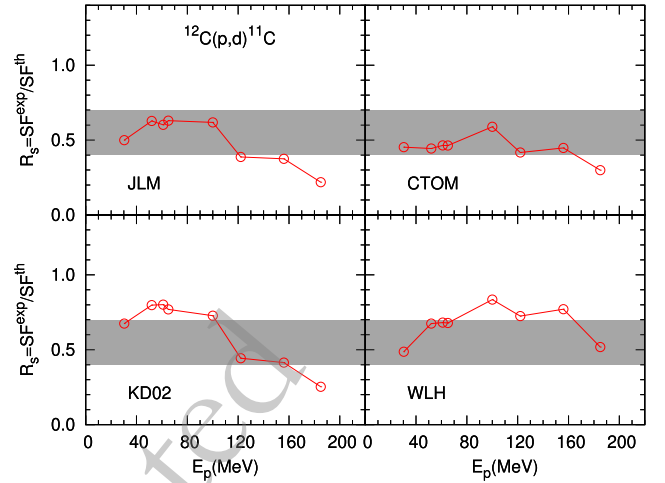
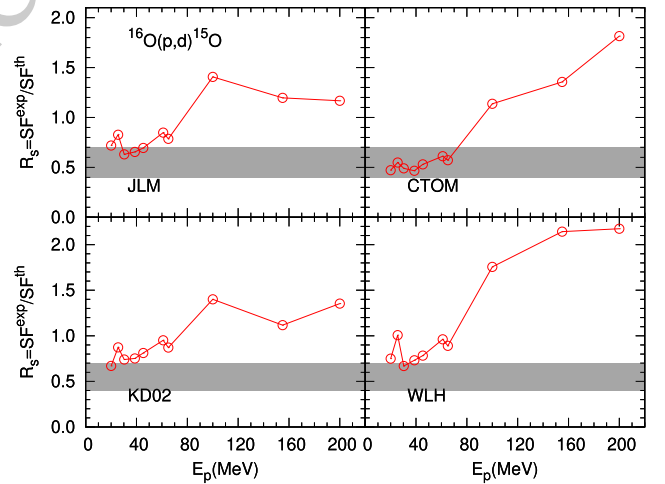
Target	$E_p/\text{MeV}$	$SF^{exp}$				
		JLM	CTOM	KD02	WLH	
$^{12}\text{C}$	30.3	1.722	1.561	1.677	2.326	
	51.93	2.163	1.528	2.326	2.751	
	61	2.075	1.600	2.347	2.761	
	65	2.170	1.598	2.339	2.651	
	100	2.131	2.029	2.877	2.507	
	122	1.335	1.437	2.498	1.529	
	156	1.291	1.542	2.656	1.428	
	185	0.753	1.030	1.784	0.871	
	$^{16}\text{O}$	20	1.324	0.869	1.380	1.234
		25.52	1.523	1.010	1.855	1.608
30.3		1.161	0.903	1.232	1.364	
38.63		1.205	0.858	1.348	1.385	
45.34		1.279	0.977	1.441	1.495	
61		1.563	1.127	1.772	1.752	
65		1.447	1.054	1.640	1.605	
100		2.591	2.094	3.234	2.580	
155		2.203	2.498	3.947	2.058	
200		2.150	3.344	4.005	2.492	
$^{28}\text{Si}$	33.6	2.816	2.139	3.883	3.820	
	51.93	3.132	2.213	3.660	3.980	
	65	2.412	1.592	2.320	3.119	
	135	0.879	0.989	1.755	1.104	
	185	0.869	1.158	1.923	1.014	
	$^{40}\text{Ca}$	27.5	2.829	2.031	2.854	2.974
30.3		3.417	2.594	3.399	3.667	
33.6		4.299	3.238	4.498	4.691	
40		4.072	3.131	4.328	4.701	
51.93		3.749	2.796	3.928	4.343	
65		2.697	1.950	2.746	3.041	
156		3.199	3.678	4.656	2.926	
185		2.703	3.850	4.589	2.569	
200		2.091	2.225	3.986	2.100	

**Table 3.** List of the shell model predicted spectroscopic factors,  $SF^{th}$  and interactions used in shell model calculations.

Reaction	$nlj$	$SF^{th}$	Interaction
$^{12}C_{g.s.}(p,d)^{11}C_{g.s.}$	0p3/2	3.447	WBT
$^{16}O_{g.s.}(p,d)^{15}O_{g.s.}$	0p1/2	1.842	WBT
$^{28}Si_{g.s.}(p,d)^{27}Si_{g.s.}$	0d5/2	3.887	USD
$^{40}Ca_{g.s.}(p,d)^{39}Ca_{g.s.}$	0d3/2	3.885	SPDF-M

SFs measured in  $(e, e'p)$  reactions, which are free from the uncertainties of OMPs and are thus deemed to be more reliable, lie within the range between 0.4 and 0.7 approximately [47, 61]. Therefore, it is expected that SFs derived from a self-consistent analysis are quenched by a common factor about  $0.55 \pm 0.10$ , independent of whether the reaction is nucleon adding or removing, whether a neutron or proton is transferred, the mass of the nucleus, the reaction type, or angular momentum transfer [47, 61]. In this work, we assess the stability of  $SF^{exp}$  extracted from  $(p, d)$  reactions by comparing  $R_s$  with the systematics of  $(e, e'p)$  reactions. The  $R_s$  values as a function of the incident energy for different targets are plotted in Figs. 2-5. The open circles represent the results calculated by microscopic OMPs and phenomenological OMPs.

Overall, one observes that the  $R_s$  values under different OMPs show no significant incident energy dependence when  $E < 70$  MeV, which is consistent with the results of Ref. [39]. However, there are only three points for  $^{28}Si$ . And the  $R_s$  values of  $^{40}Ca$  scatter considerably, although they are obtained using the consistent methodology with which all reactions are analyzed with the same procedure without free parameters. New precision measurements will be helpful. Satisfactorily, the results with CTOM are in good consistency with the systematics of  $(e, e'p)$  reactions at low energies, which is also the energy range of most previous systematic analyses to  $(d, p)$  and  $(p, d)$  reactions [1, 3, 38, 39]. It would thus be worthwhile to reanalyse previous work by applying CTOM. However, the situation becomes more complex with the beam energy increase. To gain a clear insight, the  $R_s/SF$  values are fitted by a linear function on the incident energies. The results are listed in Table 4. Figure 6 shows the slope parameters from linear fits of spectroscopic factors obtained by different OMPs. As can be seen, the  $R_s/SF$  values obtained by phenomenological OMP KD02 and old microscopic OMP JLM exhibit clear decreases for  $^{12}C$ ,  $^{28}Si$  and  $^{40}Ca$ , and an obvious increase for  $^{16}O$ , with incident energy increase. It is inconsistent with the results in knockout reactions, where no strong incident energy dependence in the  $R_s$  values within the wide energy range(43-2100 MeV/nucleon) [40]. This significant energy dependence is strongly reduced when new microscopic OMPs are employed in the calculations, except for  $^{16}O$ . In fact, there are noticeable discrepancies of the ex-

**Fig. 2.** (color online) Reduction factors of the single neutron spectroscopic factors for  $^{12}C_{g.s.}(p,d)^{11}C_{g.s.}$  with different OMPs indicated in the figures. The grey area represents the totality of the bulk of  $R_s$  for the  $(e, e'p)$  from Ref. [47, 61] to guide the eye.**Fig. 3.** (color online) Same as Fig. 2 but for  $^{16}O_{g.s.}(p,d)^{15}O_{g.s.}$ .

perimental SF values calculated by new microscopic OMPs compared with those resulted from KD02 and JLM when  $E \geq 100$  MeV/nucleon, especially for  $^{16}O$  and  $^{40}Ca$ .

As stated above, there is no significant difference in the extraction of SF values between the semi-microscopic potential JLM and the phenomenological potential KD. This is not surprising, since neutron capture rate calculations using the KD02 and JLM also give similar results [62]. Although JLM has showed good predictive power for scattering and transfer reactions, its phenomenological aspect makes its precision hard to improve beyond the use of better nuclear structure input, and it relies on simplified nuclear matter calculations with old-fashioned bare interactions.

These new microscopic OMPs, CTOM and WLH,

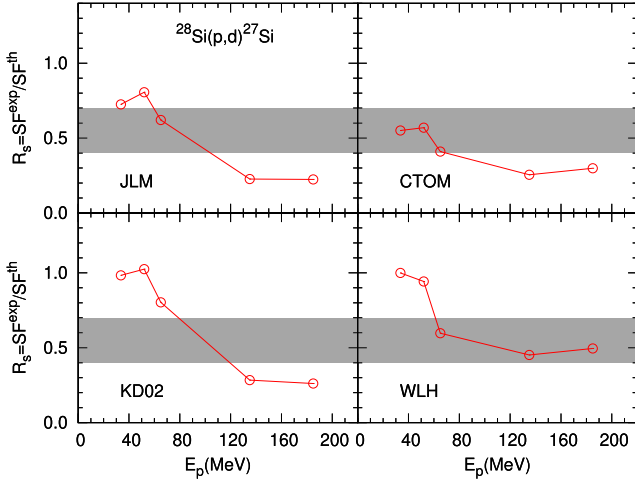


Fig. 4. (color online) Same as Fig. 2 but for  $^{28}\text{Si}_{g.s.}(p,d)^{27}\text{Si}_{g.s.}$ .

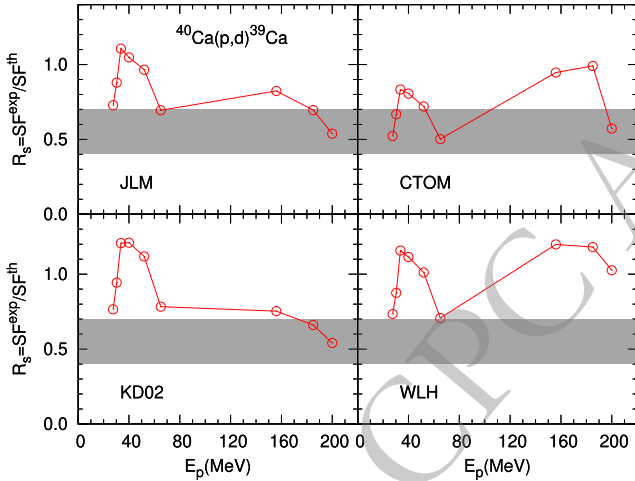


Fig. 5. (color online) Same as Fig. 2 but for  $^{40}\text{Ca}_{g.s.}(p,d)^{39}\text{Ca}_{g.s.}$ .

constructed from modern nuclear matter calculations may provide an anticipated prospect. Obviously, CTOM potential parameters can provide credible SFs with a smaller energy dependence and better consistency with results of  $(e, e'p)$  reactions at low energy region. Results calculated by WLH tend to be similar but generally larger than those using CTOM parameters. However, the nuclear matter approach omits surface effects, resonances as well as spin-orbit interactions, and tends to produce an overly absorptive imaginary term at high energies. These shortcomings may lead to they can not perform well at higher energies. Another discrepancy of the SFs happened on double-magic nuclei. Ref. [63] shows that for double-magic nuclei, the important contribution to SF almost comes from the internal nuclear region, while for other nuclei, the contribution comes from the surface area maybe not neglected. When a systematic potential derived from a large amount of elastic scattering data extrapolated to other nuclei or other energy regions, it is usually can reasonably reproduce these experimental data,

Table 4. Spectroscopic factors slope parameters for different optical model potentials.

Target	slope ( $\text{MeV}^{-1}$ )			
	JLM	CTOM	WLH	KD02
$^{12}\text{C}$	-0.008	-0.002	0.001	-0.012
$^{16}\text{O}$	0.006	0.014	0.017	0.007
$^{28}\text{Si}$	-0.016	-0.008	-0.013	-0.022
$^{40}\text{Ca}$	-0.007	0.003	0.005	-0.010

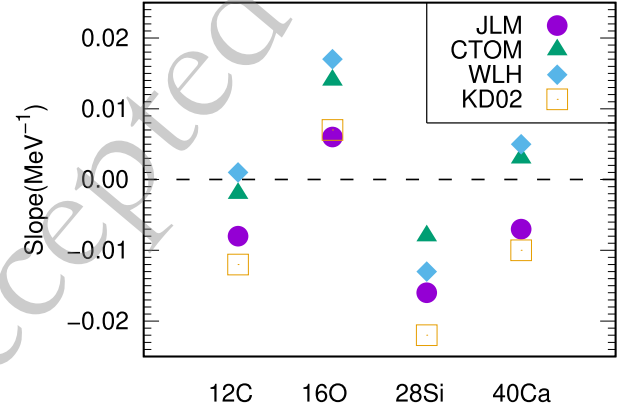


Fig. 6. (color online) A summary of spectroscopic factor slope parameters across different optical parameters.

but it can not provide satisfactorily results for double-magic nuclei, because of their special properties. It is well-known OMPs with doubly-magic nuclei do not follow the systematics of OMPs established for other nuclei due to the relatively larger excitation energies of their first few excited states [64, 65]. Moreover, We note that the fitting of CTOM lacks the nucleon elastic scattering data for light nuclei at high energies. In fact, the CTOM predictions tend to underestimate the data for the differential cross section of  $^{12}\text{C}$ - $^{40}\text{Ca}$  above 120 MeV. However, these underestimations become more serious in  $^{16}\text{O}$  and  $^{40}\text{Ca}$ .

Note that, although ADWA is generally regarded as a reliable tool for describing transfer reactions in the non-relativistic energy region, previous applications have focused on the range of  $< 70$  MeV/nucleon. In Ref. [66], the discrepancy between the ADWA and Faddeev models was found to be much larger at 50 MeV/nucleon than at 28 MeV/nucleon in  $^{48}\text{Ca}(d,p)^{49}\text{Ca}$  case, which would lead to larger SFs at higher energies, consistent with the findings of the present work. A systematic analysis by solving the Faddeev-AGS equations would be interesting and may help to further understand the systematic discrepancy.

#### IV. SUMMARY

Optical model potentials are important inputs in direct nuclear reaction calculations and great advances have

been achieved in recent years in OMPs. In this paper, a systematic analysis is made with 32 sets of angular distributions of ( $p, d$ ) reactions on 4 even–even nuclei with energies from 18 to 200 MeV/nucleon, within the ADWA framework. We investigate separately the effects of different OMPs on nuclear structure information derived from transfer reactions. Three microscopic and one phenomenological OMPs are used in the analysis. Among them, JLM relies on simplified nuclear matter calculations with old-fashioned bare interactions, while CTOM and WLH are recently proposed, which are based on modern nuclear matter calculations. We find spectroscopic values extracted from ( $p, d$ ) reactions by using JLM and phenomenological KD02 potential exhibit a strong energy dependence on beam energies. The incident energy dependence is suppressed when new microscopic OMPs, CTOM and WLH, are employed except for  $^{16}\text{O}$ . Specially, spectroscopic factors extracted using the systematic microscopic optical potential CTOM based on the Dirac-Brueckner-Hartree-Fock theory are consistent with results obtained from ( $e, e'p$ ) measurements, except  $^{16}\text{O}$  and  $^{40}\text{Ca}$  at high energies ( $\geq 100$  MeV), calling for an exact treatment of double-magic nuclei. The results obtained by using pure microscopic optical potential WLH based on EFT theory show the same trend but are generally higher than CTOM. Our results suggest the new microscopic optical potential based on modern nuclear mat-

ter approaches can effectively improve the extraction of the SFs and its reduction factors below 70 MeV/nucleon, compared with JLM folding potentials and phenomenological potentials KD02. Our work suggests that ongoing microscopic optical potentials, which are based on more fundamental principles of nuclear interactions, allow us to get more reliable nuclear structure information than phenomenological OMPs and traditional semi-microscopic OMPs. Unfortunately, the CTOM and WLH potential parameters can not give satisfactorily results for double-magic nuclei or at high energies. The quality of describing the properties of nuclei from optical potentials derived within the nuclear matter approach must be assessed by comparisons to experimental data. Our work may also be valuable for such purposes.

The relatively simple model ADWA is used in this work in order to compare the reduction factors. More rigorous theories, such as the continuum discretized coupled channels method (CDCC) and the Faddeev-AGS equations, may be helpful to explain the systematic discrepancy at different energies. In addition, effects of non-locality of the nucleon potentials and core excitations may not be neglected at higher energies. HF calculations are used in this work to constrain the parameters for the parameters, which may not be optimum for some nuclei. Further study on better methodology for the calculations will also be interesting and anticipated.

## References

- [1] X. D. Liu, M. A. Famiano, W. G. Lynch, M. B. Tsang, and J. A. Tostevin, *Phys. Rev. C* **69**, 064313 (2004)
- [2] J. Lee, J. A. Tostevin, and B. A. Brown, *Phys. Rev. C* **73**, 044608 (2006)
- [3] J. Lee, M. B. Tsang, and W. G. Lynch, *Phys. Rev. C* **75**, 064320 (2007)
- [4] J.-P. Jeukenne, A. Lejeune, and C. Mahaux, *Phys. Rev. C* **16**, 80 (1977)
- [5] E. Bauge, J. P. Delaroche, and M. Girod, *Phys. Rev. C* **58**, 1118 (1998)
- [6] R. R. Xu, Z. Y. Ma, Y. Zhang, Y. Tian, E. N. E. van Dalen, and H. Mütter, *Phys. Rev. C* **94**, 034606 (2016)
- [7] T. R. Whitehead, Y. Lim, and J. W. Holt, *Phys. Rev. Lett.* **127**, 182502 (2021)
- [8] A. Koning and J. Delaroche, *Nuclear Physics A* **713**, 231 (2003)
- [9] N. K. Glendenning, *Direct Nuclear Reactions* (World Scientific, Singapore, 2004).
- [10] T. Aumann, C. Barbieri, and D. B., *et al.*, *Progress in Particle and Nuclear Physics* **118**, 103847 (2021)
- [11] H. C. Lee, *Survey of neutron spectroscopic factors and asymmetry dependence of neutron correlations in transfer reactions*, Ph.D. thesis, Michigan State University, USA (2010).
- [12] F. M. Nunes, A. Deltuva, and J. Hong, *Phys. Rev. C* **83**, 034610 (2011)
- [13] D. Y. Pang and A. M. Mukhamedzhanov, *Phys. Rev. C* **90**, 044611 (2014)
- [14] A. E. Lovell, F. M. Nunes, J. Sarich, and S. M. Wild, *Phys. Rev. C* **95**, 024611 (2017)
- [15] G. B. King, A. E. Lovell, and F. M. Nunes, *Phys. Rev. C* **98**, 044623 (2018)
- [16] N. Timofeyuk and R. Johnson, *Progress in Particle and Nuclear Physics* **111**, 103738 (2020)
- [17] J. Lee, M. B. Tsang, W. G. Lynch, M. Horoi, and S. C. Su, *Phys. Rev. C* **79**, 054611 (2009)
- [18] J. Lee, M. B. Tsang, D. Bazin, D. Coupland, V. Henzl, D. Henzlova, M. Kilburn, W. G. Lynch, A. M. Rogers, A. Sanetullaev, A. Signoracci, Z. Y. Sun, M. Youngs, K. Y. Chae, R. J. Charity, H. K. Cheung, M. Famiano, S. Hudan, P. O'Malley, W. A. Peters, K. Schmitt, D. Shapira, and L. G. Sobotka, *Phys. Rev. Lett.* **104**, 112701 (2010)
- [19] R. C. Johnson and P. J. R. Soper, *Phys. Rev. C* **1**, 976 (1970)
- [20] S. Dickey, J. Kraushaar, and M. Rumore, *Nuclear Physics A* **391**, 413 (1982)
- [21] S. Nakayama and Y. Watanabe, *Journal of Nuclear Science and Technology* **53**, 89 (2016)
- [22] M. Yahiro, K. Ogata, T. Matsumoto, and K. Minomo, *Progress of Theoretical and Experimental Physics* **2012**, 01A (2012)
- [23] N. B. Nguyen, F. M. Nunes, and R. C. Johnson, *Phys. Rev. C* **82**, 014611 (2010)
- [24] X. Y. Yun, D. Y. Pang, Y. P. Xu, Z. Zhang, R. R. Xu, Z. Y. Ma, and C. X. Yuan, *SCIENCE CHINA Physics, Mechanics & Astronomy* **63**, 222011 (2020)
- [25] W. L. J. Lee, M. B. Tsang, Neutron spectroscopic factors

- from transfer reactions, arXiv: nucl-ex/0511024.
- [26] Experimental nuclear reaction data(exfor/csirs), [DB(DB/OL)].
- [27] J. Lee, S. Mark, P. Portner, and R. Moore, *Nuclear Physics A* **106**, 357 (1967)
- [28] J. R. Comfort and B. C. Karp, *Phys. Rev. C* **21**, 2162 (1980)
- [29] D. A. du texte Bachelier, M. Bernas, I. Brissaud, C. Detraz, and P. Radvanyi, *Nuclear Physics* **126**, 60 (1969)
- [30] A. Ingemarsson and G. Tibell, *Physica Scripta* **10**, 159 (1974)
- [31] R. Abegg, D. A. Hutcheon, C. A. Miller, L. Antonuk, J. M. Cameron, G. Gaillard, J. M. Greben, P. Kitching, R. P. Liljestrang, W. J. McDonald, W. C. Olsen, G. M. Stinson, J. Tinsley, and P. D. Kunz, *Phys. Rev. C* **39**, 65 (1989)
- [32] J. Källne and B. Fagerström, *Physica Scripta* **11**, 79 (1975)
- [33] R. Johnson and P. Tandy, *Nuclear Physics A* **235**, 56 (1974)
- [34] J. S. Petler, M. S. Islam, R. W. Finlay, and F. S. Dietrich, *Phys. Rev. C* **32**, 673 (1985)
- [35] J. A. Tostevin and A. Gade, *Phys. Rev. C* **103**, 054610 (2021)
- [36] Y. Z. Sun, S. T. Wang, and Z. Y. Sun, *et al.*, *Phys. Rev. C* **104**, 014310 (2021)
- [37] Y. Z. Sun, S. T. Wang, Y. P. Xu, D. Y. Pang, J. G. Li, C. X. Yuan, L. F. Wan, Y. Qiao, Y. Q. Wang, and X. Y. Chen, *Phys. Rev. C* **106**, 034614 (2022)
- [38] Y. Xu, D. Pang, and X. Y., *et al.*, *Physics Letters B* **790**, 308 (2019)
- [39] J. Manfredi, J. Lee, and A. M. Rogers, *et al.*, *Phys. Rev. C* **104**, 024608 (2021)
- [40] Y.-P. Xu, D.-Y. Pang, C.-X. Yuan, and X.-Y. Yun, *Chinese Physics C* **46**, 064102 (2022)
- [41] B. Alex Brown, *Phys. Rev. C* **58**, 220 (1998)
- [42] J. Tostevin, University of Surrey version of the code twofnr (of m. toyama, m. igarashi and n. kishida) and code front (private communication), (1977).
- [43] B.A.Brown, A.Etchegoyen, and W.D.M.Rae, Oxbash, the oxford university- buenos aires-msu shell model code, (1985).
- [44] A. E. L. Dieperink and T. d. Forest, *Phys. Rev. C* **10**, 543 (1974)
- [45] M. B. Tsang, J. Lee, and S. C. Su, *et al.*, *Phys. Rev. Lett.* **102**, 062501 (2009)
- [46] F. Flavigny, A. Gillibert, and L. Nalpas, *et al.*, *Phys. Rev. Lett.* **110**, 122503 (2013)
- [47] B. P. Kay, J. P. Schiffer, and S. J. Freeman, *Phys. Rev. Lett.* **111**, 042502 (2013)
- [48] F. Flavigny, N. Keeley, and A. Gillibert, *et al.*, *Phys. Rev. C* **97**, 034601 (2018)
- [49] A. Gade, P. Adrich, D. Bazin, M. D. Bowen, B. A. Brown, C. M. Campbell, J. M. Cook, T. Glasmacher, P. G. Hansen, K. Hosier, S. McDaniel, D. McGlinchery, A. Obertelli, K. Siwek, L. A. Riley, J. A. Tostevin, and D. Weisshaar, *Phys. Rev. C* **77**, 044306 (2008)
- [50] E. C. Simpson and J. A. Tostevin, *Phys. Rev. C* **79**, 024616 (2009)
- [51] J. A. Tostevin and A. Gade, *Phys. Rev. C* **90**, 057602 (2014)
- [52] R. J. Charity, L. G. Sobotka, and J. A. Tostevin, *Phys. Rev. C* **102**, 044614 (2020)
- [53] J. Díaz-Cortés, J. Benlliure, and J. R.-S., *et al.*, *Physics Letters B* **811**, 135962 (2020)
- [54] L. Atar, S. Paschalis, and C. Barbieri, *et al.*, *Phys. Rev. Lett.* **120**, 052501 (2018)
- [55] M. Gómez-Ramos and A. Moro, *Physics Letters B* **785**, 511 (2018)
- [56] S. Kawase, T. Uesaka, and T. L. T., *et al.*, *Progress of Theoretical and Experimental Physics* **2018**, (2018)
- [57] N. T. T. Phuc, K. Yoshida, and K. Ogata, *Phys. Rev. C* **100**, 064604 (2019)
- [58] M. Holl, V. Panin, and H. A.-P., *et al.*, *Physics Letters B* **795**, 682 (2019)
- [59] C. A. Bertulani, A. Idini, and C. Barbieri, *Phys. Rev. C* **104**, L061602 (2021)
- [60] J. Li, C. A. Bertulani, and F. Xu, *Phys. Rev. C* **105**, 024613 (2022)
- [61] G. Kramer, H. Blok, and L. Lapikas, *Nuclear Physics A* **679**, 267 (2001)
- [62] C. Hebborn, F. M. Nunes, G. Potel, W. H. Dickhoff, J. W. Holt, M. C. Atkinson, R. B. Baker, C. Barbieri, G. Blanchon, M. Burrows, R. Capote, P. Danielewicz, M. Dupuis, C. Elster, J. E. Escher, L. Hlophe, A. Idini, H. Jayatissa, B. P. Kay, K. Kravvaris, J. J. Manfredi, A. Mercenne, B. Morillon, G. Perdikakis, C. D. Pruitt, G. H. Sargsyan, I. J. Thompson, M. Vorabbi, and T. R. Whitehead, *Journal of Physics G: Nuclear and Particle Physics* **50**, 060501 (2023)
- [63] N. K. Timofeyuk, *Journal of Physics G: Nuclear and Particle Physics* **41**, 094008 (2014)
- [64] R. Varner, W. Thompson, T. McAbee, E. Ludwig, and T. Clegg, *Physics Reports* **201**, 57 (1991)
- [65] D. Y. Pang, P. Roussel-Chomaz, H. Savajols, R. L. Varner, and R. Wolski, *Phys. Rev. C* **79**, 024615 (2009)
- [66] F. M. Nunes and A. Deltuva, *Phys. Rev. C* **84**, 034607 (2011)